

## Contrasting the magnetic response between a magnetic glass and a reentrant spin glass

S. B. Roy and M. K. Chattopadhyay

*Magnetic and Superconducting Materials Section, Raja Ramanna Centre for Advanced Technology, Indore 452013, India*

(Received 5 December 2008; revised manuscript received 23 January 2009; published 27 February 2009)

Magnetic glass is a recently identified phenomenon in various classes of magnetic systems undergoing a first-order magnetic phase transition. We shall highlight here a few experimentally determined characteristics of magnetic glass and the relevant set of experiments, which will enable to distinguish a magnetic glass unequivocally from the well-known phenomena of spin glass and reentrant spin glass.

DOI: [10.1103/PhysRevB.79.052407](https://doi.org/10.1103/PhysRevB.79.052407)

PACS number(s): 75.30.Kz

It has been shown recently that in many magnetic systems a kinetic arrest of the first-order ferromagnetic (FM) to anti-ferromagnetic (AFM) phase transition leads to a nonequilibrium magnetic state with a configuration of FM and AFM clusters frozen randomly in experimental time scale.<sup>1-7</sup> The dynamics of this nonequilibrium magnetic state is very similar to that of a structural glass,<sup>8</sup> and analogically, this new magnetic state is named magnetic glass (MG).<sup>2,7,9</sup> The results emerging from disparate classes of magnetic systems starting from alloys and intermetallic compounds<sup>1-3,6,7,9</sup> to manganite systems showing colossal magnetoresistance (CMR) (Refs. 3-5) suggest that this magnetic-glass phenomenon is independent of the underlying microscopic nature of magnetic interactions. Analogous to the structural glasses, the MG can undergo devitrification with the change in temperature ( $T$ ).<sup>10,11</sup>

Competition between AFM and FM interactions plays the central role in spin glass (SG) and reentrant spin glass (RSG).<sup>12,13</sup> In SG this competition is so strong that none of the long-range magnetic orders is established; instead it gives rise to a random spin configuration frozen in time.<sup>13</sup> In RSG, long-range magnetic order (FM or AFM) appears in certain  $T$  regime. However, the competing interactions introduce some frustration among the set of spins, which ultimately leads to the partial or total breakdown of the higher  $T$  FM or AFM state to a SG-like state at the lowest  $T$ .<sup>12,13</sup> The spin configuration of this lower  $T$  RSG state consists of individual spins (or small spin clusters) frozen randomly in the microscopic scale with<sup>14</sup> or without<sup>15</sup> a trace of long-range FM order along the direction of the applied magnetic field ( $H$ ).

The onset of both of these nontrivial MG and RSG states is accompanied by distinct  $H$  and  $T$  history dependence of bulk magnetic response, i.e., thermomagnetic irreversibilities (TMIs) and metastability, which at first sight can appear to be quite similar in nature. Such TMI and metastability are very well studied experimental observables in SG and RSG systems,<sup>12,13</sup> and they are regularly used for initial identification of SG and RSG behaviors in a new magnetic system. The main aim of the present work is to carefully study and compare the TMI and metastability associated with the MG and RSG behaviors. We shall then highlight the identifiable features in such experimental observables, which will enable to distinguish a MG unequivocally from RSG.

For our comparative study we have chosen a well studied MG system  $\text{Ce}(\text{Fe}_{0.96}\text{Ru}_{0.04})_2$  (Refs. 2 and 16) and a canonical RSG system  $\text{Au}_{82}\text{Fe}_{18}$  alloy.<sup>12,13</sup> The FM-RSG transition

in AuFe alloys above the percolation concentration of 15% Fe has been studied in great detail through both bulk properties and microscopic measurements.<sup>17</sup> Various theoretical models have been proposed to understand these experimental results.<sup>14,15</sup> In  $\text{Ce}(\text{Fe}_{0.96}\text{Ru}_{0.04})_2$ , the low  $T$  state is AFM in zero and relatively low ( $\leq 10$  kOe) applied  $H$ .<sup>2,16</sup> In the presence of an applied field  $H > 10$  kOe, the first-order FM-AFM transition in  $\text{Ce}(\text{Fe}_{0.96}\text{Ru}_{0.04})_2$  gets kinetically arrested giving rise to a MG state.<sup>2</sup> We shall now present below the contrasting TMI and metastabilities associated with the RSG behavior in  $\text{Au}_{82}\text{Fe}_{18}$  and MG behavior in  $\text{Ce}(\text{Fe}_{0.96}\text{Ru}_{0.04})_2$ .

The details of the preparation and characterization of the  $\text{Ce}(\text{Fe}_{0.96}\text{Ru}_{0.04})_2$  and  $\text{Au}_{82}\text{Fe}_{18}$  samples used here can be found in Refs. 16 and 18, respectively. The  $\text{Au}_{82}\text{Fe}_{18}$  sample, however, was freshly annealed at 800 °C for 6 h and quenched in liquid nitrogen before starting the present experimental cycle. Bulk magnetization measurements were made with a commercial vibrating sample magnetometer (Quantum Design, USA). We use three experimental protocols, zero field cooled (ZFC), field cooled cooling (FCC), and field cooled warming (FCW), for magnetization ( $M$ ) measurements. In the ZFC mode the sample is cooled to the lowest measured  $T$  before the applied  $H$  is switched on, and the measurement is made while warming up the sample. In the FCC mode the applied  $H$  is switched on in the  $T$  regime above the FM-AFM transition temperature in the case of  $\text{Ce}(\text{Fe}_{0.96}\text{Ru}_{0.04})_2$  and FM-RSG transition temperature in the case of  $\text{Au}_{82}\text{Fe}_{18}$ , and the measurement is made while cooling across the transition temperature to the lowest measured  $T$ . After completion of measurement in the FCC mode, the data points are taken again in the presence of same applied  $H$  while warming up the sample. This is called FCW mode. A fixed rate of  $T$  variation of 1 K/min has been used all throughout the present study.

The main frame of Fig. 1 presents the  $M$  versus  $T$  plot of  $\text{Au}_{82}\text{Fe}_{18}$  alloy in  $H=500$  Oe, obtained under the ZFC, FCC, and FCW modes. The value of Curie temperature ( $T_C \approx 155$  K) estimated from the point of inflection in the  $M$ - $T$  curve matches well with the earlier reported value in the literature.<sup>17</sup> The onset of the FM-RSG transition is marked by a small but distinct maximum in the  $M$ - $T$  curve at a temperature  $T_M \approx 50$  K. Then at a further lower temperature ( $T_{\text{irrv}}$ ), there is a sharp drop in the ZFC  $M$ - $T$  curve accompanied by a clear bifurcation of the ZFC and FC  $M(T)$  curves. This maximum in  $M(T)$  and the onset of strong TMI at  $T_{\text{irrv}}$  are the hallmarks of RSG behavior.<sup>12</sup> Both these features are explained within a mean-field theory of second-

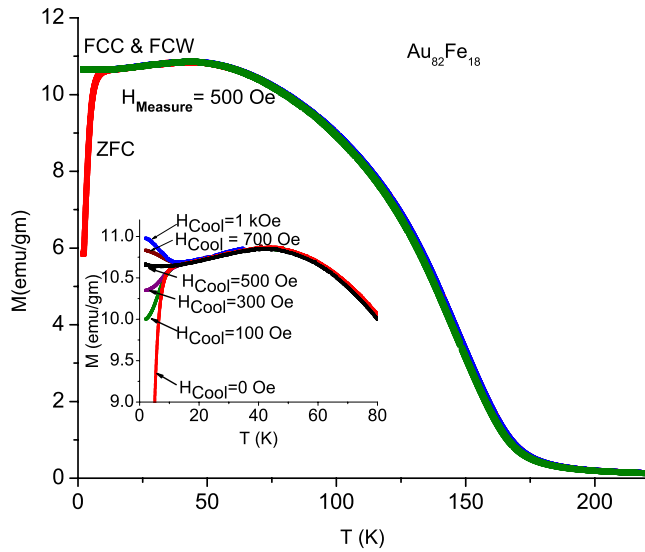


FIG. 1. (Color online)  $M$  vs  $T$  plot for  $\text{Au}_{82}\text{Fe}_{18}$  obtained with ZFC, FCC, and FCW protocols with  $H=500$  Oe. The inset shows  $M$  vs  $T$  plot obtained under an experimental protocol of cooling and heating in unequal field with  $H_{\text{measure}}=500$  Oe. See text for details.

order phase transition.<sup>14</sup> There is also an alternative viewpoint, where the maximum at  $T_M$  is envisaged as due to the onset of random freezing of isolated Fe clusters in  $\text{Au}_{82}\text{Fe}_{18}$ , which in turn creates a random internal field acting on the infinite FM cluster and leading to a complete breakdown of the long-range FM order into a spin-glass state at a lower  $T$ .<sup>15</sup> Note that in the main frame of Fig. 1 the  $M$ - $T$  curves obtained under the FCC and FCW protocols completely overlap, and this is in consonance with both types of theoretical pictures.<sup>14,15</sup> With the increase in  $H$ ,  $T_{\text{irrv}}$  decreases and the  $M$ - $T$  curve with  $H=5$  kOe [see the mainframe of Fig. 2(b)] resembles that of a standard FM with no trace of FM-RSG transition at least down to 2 K.

The mainframe of Fig. 2(a) presents the  $M$  versus  $T$  plot of  $\text{Ce}(\text{Fe}_{0.96}\text{Ru}_{0.04})_2$  in  $H=5$  kOe, obtained under the ZFC, FCC, and FCW modes. Note that here the  $M_{\text{ZFC}}(T)$  merges with  $M_{\text{FCW}}(T)$  at all measured  $T$ . A sharp rise (fall) in  $M$  in ZFC (FCC) path [see Fig. 2(a)] at temperatures  $T_{\text{NW}}$  ( $T_{\text{NC}}$ ) around 65 K marks the onset of AFM-FM (FM-AFM) transition while warming (cooling).<sup>16</sup> The distinct thermal hysteresis between  $M_{\text{FCC}}(T)$  and  $M_{\text{ZFC}}(T)$  [or  $M_{\text{FCW}}(T)$ ] in the transition region arises due to the first-order nature of the FM-AFM phase transition in  $\text{Ce}(\text{Fe}_{0.96}\text{Ru}_{0.04})_2$ . The endpoint of the thermal hysteresis while cooling (warming) represents the limit of supercooling  $T^*$  (superheating  $T^{**}$ ) across the first-order phase transition.<sup>16</sup> Below (above)  $T^*$  ( $T^{**}$ ) the system is in the equilibrium AFM (FM) state.

In the FCC mode above a critical applied  $H$  of 10 kOe, the FM-AFM transition gets kinetically arrested leading to the formation of the MG state.<sup>2</sup> This behavior is shown in the mainframe of Fig. 3 in the  $M$  vs  $T$  plot of  $\text{Ce}(\text{Fe}_{0.96}\text{Ru}_{0.04})_2$  in a field of 20 kOe. The conversion to low- $T$  AFM state is not completed in the FCC mode. While warming up part devitrification of the MG state (to equilibrium AFM state) occurs and the system eventually reaches back to the higher  $T$  FM state. In contrast, in the ZFC mode the applied  $H$  is switched

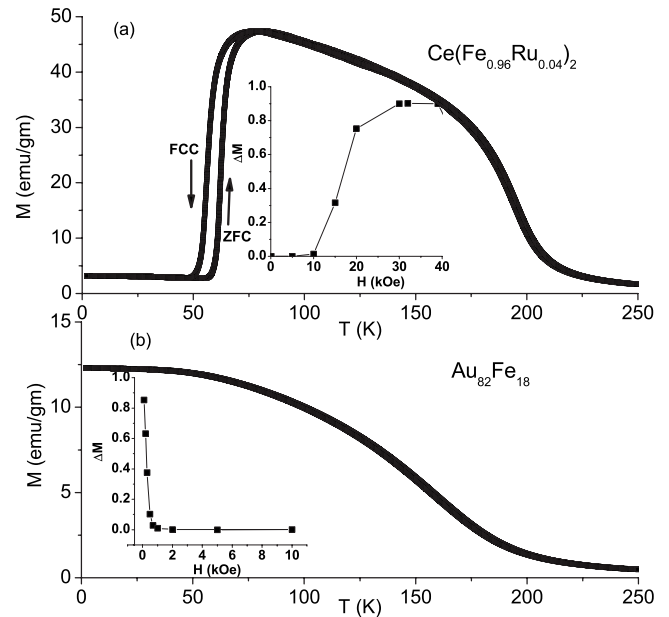


FIG. 2.  $M$  vs  $T$  plots for (a)  $\text{Ce}(\text{Fe}_{0.96}\text{Ru}_{0.04})_2$  and (b)  $\text{Au}_{82}\text{Fe}_{18}$  obtained with  $H=5$  kOe. Insets of (a) and (b) show the difference  $\Delta M$  between  $M_{\text{FCC}}(T)$  and  $M_{\text{ZFC}}(T)$  [normalized with respect to  $M_{\text{FCC}}(T)$ ] as a function of  $H$  for  $\text{Ce}(\text{Fe}_{0.96}\text{Ru}_{0.04})_2$  ( $\text{Au}_{82}\text{Fe}_{18}$ ).

on at the lowest measured  $T$ , and since in  $H \leq 10$  kOe there is no formation of MG, the equilibrium AFM state can be reached and subsequently transformed with the increase in  $T$  to the FM state. All these effects give rise to interesting TMI where  $M_{\text{FCC}}(T) \neq M_{\text{FCW}}(T)$  [and  $M_{\text{ZFC}}(T)$ ] over a large  $T$  regime (see mainframe of Fig. 3). This onset of the MG state in an applied  $H$  can be compared with the recent observation of the formation of glassy state in liquid Ge under external pressure.<sup>19</sup>

In striking contrast to the TMI in the RSG state of

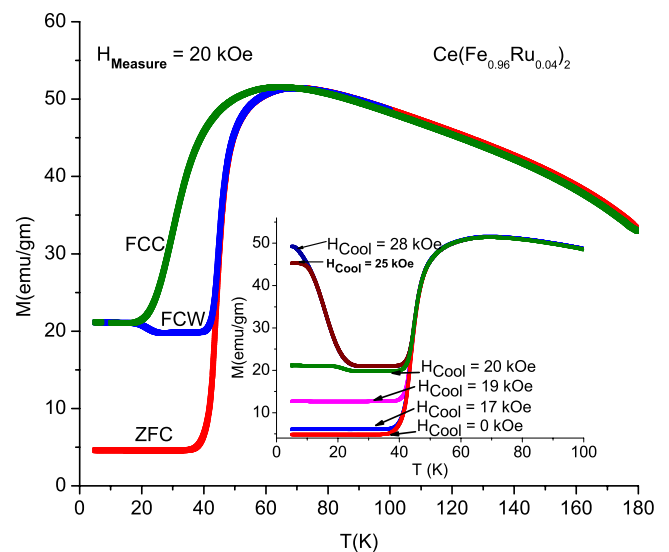


FIG. 3. (Color online)  $M$  vs  $T$  plot for  $\text{Ce}(\text{Fe}_{0.96}\text{Ru}_{0.04})_2$  obtained with ZFC, FCC, and FCW protocols with  $H=20$  kOe. The inset shows  $M$  vs  $T$  plot obtained under an experimental protocol of CHUF with  $H_{\text{measure}}=20$  kOe. See text for details.

$\text{Au}_{82}\text{Fe}_{18}$ , the TMI associated with the MG behavior in  $\text{Ce}(\text{Fe}_{0.96}\text{Ru}_{0.04})_2$  appears only above a certain critical  $H$ , and its magnitude increases with  $H$ . To highlight this difference in TMI we plot in the inset of Figs. 2(a) and 2(b)  $\Delta M = (M_{\text{FCC}}(T) - M_{\text{ZFC}}(T)) / M_{\text{FCC}}(T)$  measured at 5 K as a function of applied  $H$  both for  $\text{Ce}(\text{Fe}_{0.96}\text{Ru}_{0.04})_2$  and  $\text{Au}_{82}\text{Fe}_{18}$ . In  $\text{Au}_{82}\text{Fe}_{18}$   $\Delta M$  falls to zero rapidly as  $H$  increases to 5 kOe, while in  $\text{Ce}(\text{Fe}_{0.96}\text{Ru}_{0.04})_2$   $\Delta M$  acquires nonzero value only above  $H=10$  kOe and increases thereafter with the further increase in  $H$ .

The quenched disorder in the concerned magnetic systems influences the FM-AFM first-order transition process and introduces a landscape of transition temperature  $T_N$ .<sup>20</sup> In such systems the  $H$ - $T$  phase diagram consists of the bands of transition temperature ( $T_N$ ), supercooling and superheating limits ( $T^*$  and  $T^{**}$ ), and a kinetic arrest temperature band ( $T_K$ ) below which the system enters a MG state.<sup>1,3,10,21</sup> The correlation between the characteristic temperatures  $T_N$ ,  $T^*$  ( $T^{**}$ ), and  $T_K$  and its experimental consequences have been studied with a recently introduced experimental protocol, where the system is cooled across the transition temperature in certain applied  $H_{\text{cool}}$  and the magnetization studies are made while warming and after changing this  $H_{\text{cool}}$  isothermally to a different  $H_{\text{measure}}$  (higher or lower than  $H_{\text{cool}}$ ) at the lowest measured  $T$ .<sup>22</sup> This experimental protocol is in contrast with the standard field cooling protocols FCC and FCW, where  $H_{\text{cool}}$  and  $H_{\text{measure}}$  while warming are the same. This technique of “cooling and heating in unequal field” (CHUF) has been used to investigate the MG phenomenon in various CMR-manganite systems.<sup>22</sup> It has been shown clearly that in a kinetically arrested FM-AFM transition, while warming with  $H_{\text{measure}} > H_{\text{cool}}$  ( $H_{\text{measure}} < H_{\text{cool}}$ ) under the CHUF protocol, one observes only one sharp structure (two sharp structures) in  $M(T)$ .<sup>22</sup> We use this key result here to discern between a MG and RSG. The inset of Fig. 3 shows the results of  $M(T)$  measurements in  $\text{Ce}(\text{Fe}_{0.96}\text{Ru}_{0.04})_2$  obtained under CHUF protocol with  $H_{\text{measure}}=20$  kOe. With  $H_{\text{measure}} > H_{\text{cool}}$ , there is only one sharp rise in  $M(T)$  leading to the FM state. On the other hand, when  $H_{\text{measure}} < H_{\text{cool}}$  the  $M(T)$  drops sharply and flattens before rising sharply again to reach the FM state. With a higher value of  $H_{\text{cool}}$  the state prepared at the lowest  $T$  has a large fraction of the FM component in the MG state, and in the FCW mode  $M(T)$  drops sharply with rising  $T$  due to the devitrification of this nonequilibrium FM component. For a more detailed explanation of the origin of such distinct characteristic features associated with the MG phenomenon, the reader is referred to Ref. 22. The change in sign of the inequality between  $H_{\text{measure}}$  and  $H_{\text{cool}}$  does not lead to such distinctive characteristic features in the RSG system  $\text{Au}_{82}\text{Fe}_{18}$ , and this is shown experimentally in the  $M(T)$  study with  $H_{\text{measure}}=500$  Oe (see the inset of Fig. 1). The algebraic value of TMI around  $T_{\text{irrv}}$  changes monotonically with the change in sign of the inequality.

We shall now discuss the characteristic metastable behavior associated with the RSG and MG states. The metastable response of SG and RSG systems continues to remain a subject of active interest.<sup>23</sup> The ZFC state of these systems shows strong relaxation in magnetization, while the field cooled state does not.<sup>12,13</sup> These behaviors are exemplified in Fig. 4(a), which shows  $M$  versus time ( $t$ ) plots for  $\text{Au}_{82}\text{Fe}_{18}$

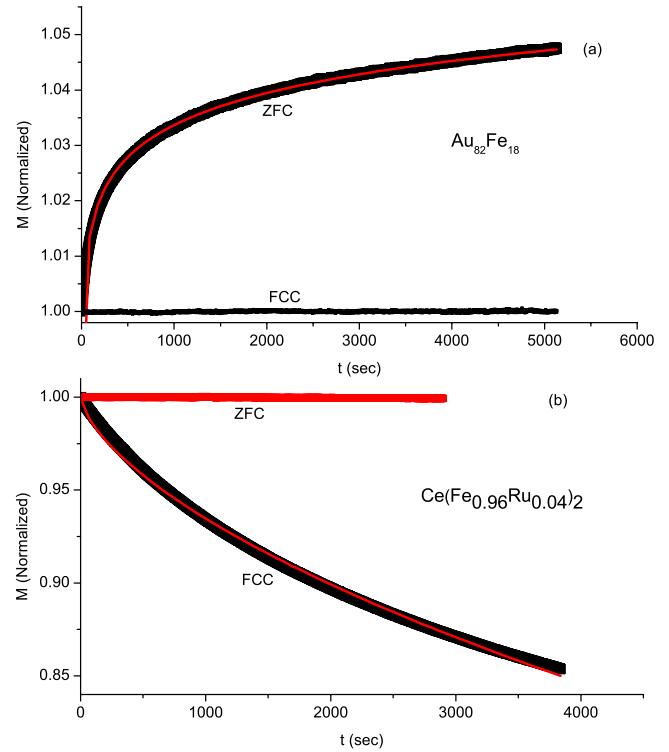


FIG. 4. (Color online)  $M$  vs time plots for (a)  $\text{Au}_{82}\text{Fe}_{18}$  at  $T=14$  K and (b)  $\text{Ce}(\text{Fe}_{0.96}\text{Ru}_{0.04})_2$  at  $T=18$  K obtained under ZFC and FCC protocols.  $M$  is normalized with respect to the initial  $M_0$  value obtained after 1 s of stabilizing at the respective measured  $T$ , which is reached with a cooling rate of 1 K/min in the “temperature no-overshoot” mode of the instrument. The relaxation data for  $\text{Au}_{82}\text{Fe}_{18}$  [ $\text{Ce}(\text{Fe}_{0.96}\text{Ru}_{0.04})_2$ ] are fitted with the equation  $M(t) = -1 + 2t^\gamma$  (stretched exponential function  $M(t) \propto \exp[-(t/\tau)^\beta]$ ).

at  $T=14$  K and  $H=100$  Oe in the ZFC and FCC state. The  $M(t)$  data in the ZFC state can be fitted with the equation  $M(t) = -1 + 2t^\gamma$ , where  $\gamma$  indicates the extent of relaxation. Higher value of  $\gamma$  means a greater degree of relaxation in the same  $t$  interval. This equation has earlier been shown to apply to the relaxation of ferromagnetic dots which interact through long-range dipolar interaction.<sup>24</sup> The obtained value of exponent  $\gamma$  in the present case is 0.004. Since the ZFC state in MG is an equilibrium state, no relaxation of  $M$  is observed there. On the other hand, entrance into the MG state along the FCC path introduces distinct glasslike relaxation and the divergence of the relaxation time with lowering in  $T$ .<sup>2,7,9</sup> To contrast such metastability with that observed in the RSG state, we present in Fig. 4(b)  $M$  vs time plot obtained for  $\text{Ce}(\text{Fe}_{0.96}\text{Ru}_{0.04})_2$  at  $T=18$  K and  $H=20$  kOe in the ZFC state and FCC state. The  $M(t)$  data in the FCC state can be fitted with the Kohlrausch-Williams-Watt stretched exponential function  $M(t) \propto \exp[-(t/\tau)^\beta]$ , where  $\tau$  is the characteristic relaxation time and  $\beta$  is a shape parameter.<sup>2</sup> The obtained value of exponent  $\beta$  here is 0.65.

The metastable nature of the FCC state in systems showing MG behavior can be supported further by showing that this state is susceptible to any energy fluctuation introduced by a  $T$  or  $H$  cycling.<sup>2,7,9</sup> Similar extensive  $T$  cycling in the FCC state of the present  $\text{Au}_{82}\text{Fe}_{18}$  sample failed to reveal any such signature of metastability.<sup>25</sup>

Summarizing the above experimental results, we identify four distinct experimental features in bulk magnetization measurements, which can be used to distinguish a magnetic-glass from a reentrant spin glass.

(i) MG arises out of the kinetic arrest of a first-order FM-AFM phase transition. This first-order transition will give rise to a distinct thermal hysteresis between the FCC and FCW magnetizations. No such thermal hysteresis is expected in the case of FM- (or AFM)-RSG transition since this is considered to be a second-order phase transition<sup>14</sup> or a gradual phase transformation.<sup>15</sup>

(ii) The TMI decreases with the increase in the applied  $H$  in RSG systems. This is just the opposite in MG, where TMI appears only above a critical applied  $H$  (the value of which will depend on the system under consideration) and increases with the increase in  $H$ .

(iii) A recently introduced experimental protocol CHUF

reveals distinct features in the  $T$  dependence of magnetization in MG, which depends on the sign of inequality between the fields applied during cooling and heating. No such features are expected for a RSG system.

(iv) ZFC state of RSG shows distinct relaxation in magnetization, while the FC state does not. The behavior observed in the MG systems is just the opposite.

In conclusion the observed magnetic-glass phenomenon in different magnetic systems is distinctly different from the well-known spin-glass and reentrant spin-glass phenomena. While the existence of the magnetic-glass systems will finally be established through microscopic studies like magnetic imaging, the experimental criteria described in this work can definitely be used for regular identification of a magnetic-glass.

The authors thank P. Chaddah for useful discussion.

- 
- <sup>1</sup>M. A. Manekar, S. Chaudhary, M. K. Chattopadhyay, K. J. Singh, S. B. Roy, and P. Chaddah, *Phys. Rev. B* **64**, 104416 (2001).
- <sup>2</sup>M. K. Chattopadhyay, S. B. Roy, and P. Chaddah, *Phys. Rev. B* **72**, 180401(R) (2005).
- <sup>3</sup>K. Kumar, A. K. Pramanik, A. Banerjee, P. Chaddah, S. B. Roy, S. Park, C. L. Zhang, and S.-W. Cheong, *Phys. Rev. B* **73**, 184435 (2006).
- <sup>4</sup>W. Wu, C. Israel, N. Hur, P. Soonyong, S.-W. Cheong, and A. De Lozane, *Nature Mater.* **5**, 881 (2006).
- <sup>5</sup>A. Banerjee, K. Mukherjee, Kranti Kumar, and P. Chaddah, *J. Phys.: Condens. Matter* **18**, L605 (2006); *Phys. Rev. B* **74**, 224445 (2006); Z. W. Ouyang, H. Nojiri, and S. Yoshii, *ibid.* **78**, 104404 (2008).
- <sup>6</sup>K. Sengupta and E. V. Sampathkumaran, *Phys. Rev. B* **73**, 020406(R) (2006); P. Kushwaha, R. Rawat, and P. Chaddah, *J. Phys.: Condens. Matter* **20**, 022204 (2008).
- <sup>7</sup>S. B. Roy, M. K. Chattopadhyay, P. Chaddah, J. D. Moore, G. K. Perkins, L. F. Cohen, K. A. Gschneidner, Jr., and V. K. Pecharsky, *Phys. Rev. B* **74**, 012403 (2006).
- <sup>8</sup>P. G. Debenedetti and F. H. Stillinger, *Nature (London)* **410**, 259 (2001).
- <sup>9</sup>V. K. Sharma, M. K. Chattopadhyay, and S. B. Roy, *Phys. Rev. B* **76**, 140401(R) (2007).
- <sup>10</sup>S. B. Roy, M. K. Chattopadhyay, A. Banerjee, P. Chaddah, J. D. Moore, G. K. Perkins, L. F. Cohen, K. A. Gschneidner, Jr., and V. K. Pecharsky, *Phys. Rev. B* **75**, 184410 (2007); M. K. Chattopadhyay, S. B. Roy, K. Morrison, J. D. Moore, G. K. Perkins, L. F. Cohen, K. A. Gschneidner, Jr., and V. K. Pecharsky, *Europhys. Lett.* **83**, 57006 (2008).
- <sup>11</sup>P. Chaddah, K. Kumar, and A. Banerjee, *Phys. Rev. B* **77**, 100402(R) (2008).
- <sup>12</sup>K. H. Binder and A. P. Young, *Rev. Mod. Phys.* **58**, 801 (1986).
- <sup>13</sup>J. A. Mydosh, *Spin Glasses* (Taylor & Francis, London, 1992).
- <sup>14</sup>M. Gabay and G. Toulouse, *Phys. Rev. Lett.* **47**, 201 (1981).
- <sup>15</sup>S. Niidera and F. Matsubara, *Phys. Rev. B* **75**, 144413 (2007).
- <sup>16</sup>S. B. Roy, G. K. Perkins, M. K. Chattopadhyay, A. K. Nigam, K. J. S. Sokhey, P. Chaddah, A. D. Caplin, and L. F. Cohen, *Phys. Rev. Lett.* **92**, 147203 (2004).
- <sup>17</sup>B. R. Coles, B. V. B. Sarkissian, and R. H. Taylor, *Philos. Mag. B* **37**, 489 (1978); B. V. B. Sarkissian, *J. Phys. F: Met. Phys.* **11**, 2191 (1981); I. A. Campbell, D. Arvanitis, and A. Fert, *Phys. Rev. Lett.* **51**, 57 (1983).
- <sup>18</sup>A. K. Gangopadhyay, S. B. Roy, and A. K. Majumdar, *Phys. Rev. B* **33**, 5010 (1986).
- <sup>19</sup>M. H. Bhat, V. Molinero, E. Soignard, V. C. Solomon, S. Sastry, and J. L. Yarger, *Nature (London)* **448**, 787 (2007).
- <sup>20</sup>Y. Imry and M. Wortis, *Phys. Rev. B* **19**, 3580 (1979).
- <sup>21</sup>P. Chaddah, A. Banerjee, and S. B. Roy, arXiv:cond-mat/0601095 (unpublished).
- <sup>22</sup>A. Banerjee, K. Kumar, and P. Chaddah, *J. Phys.: Condens. Matter* **21**, 026002 (2009); S. Dash, A. Banerjee, and P. Chaddah, *Solid State Commun.* **148**, 336 (2008).
- <sup>23</sup>K. Hioki and K. Motoya, *J. Phys. Soc. Jpn.* **74**, 1830 (2005) and references therein.
- <sup>24</sup>L. C. Sampaio, R. Hyndman, F. S. de Menezes, J. P. Jamet, P. Meyer, J. Gierak, C. Chappert, V. Mathet, and J. Ferre, *Phys. Rev. B* **64**, 184440 (2001).
- <sup>25</sup>S. B. Roy and M. K. Chattopadhyay (unpublished).